Accepted for publication in ***Environmental Pollution***

Influence of avenue-trees on air quality at the urban neighborhood scale. Part I: Quality assurance studies and turbulent Schmidt number analysis for RANS CFD simulations

Christof Gromke, Bert Blocken

Graphical abstract

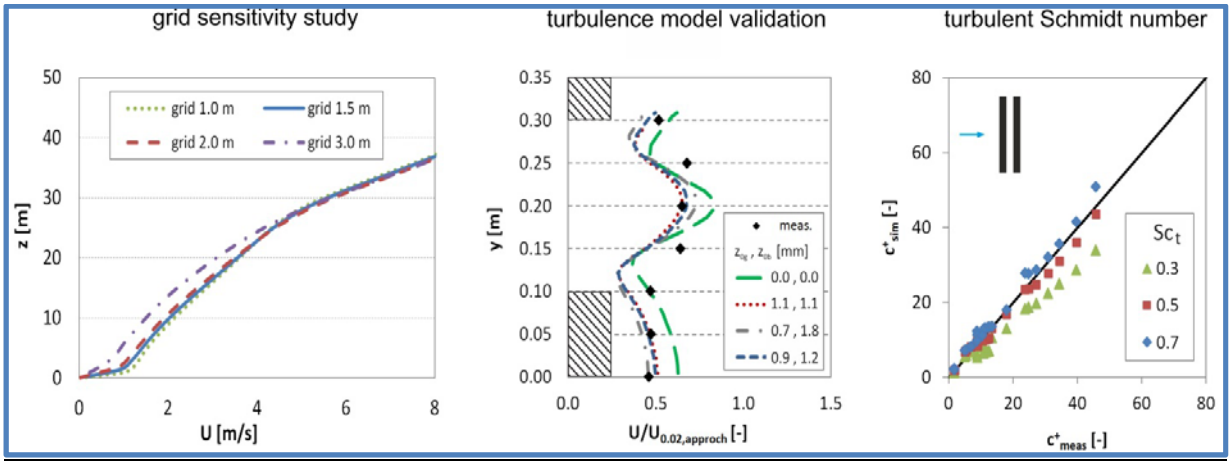

Highlights

- Validation studies for CFD of dispersion in urban areas with avenue-trees were done.
- A grid sensitivity study yielded a cell count of 20 cells per building height.
- The realizable k-ε turbulence model was validated for a generic urban configuration.
- A vegetation model was validated for flow and turbulence in tree crowns.
- An appropriate turbulent Schmidt number was determined as $Sc_t = 0.5$.

Abstract

Flow and dispersion of traffic pollutants in a generic urban neighborhood with avenue-trees were investigated with Computational Fluid Dynamics (CFD). In Part I of this two-part contribution, quality assessment and assurance for CFD simulations in urban and vegetation configurations were addressed, before in Part II flow and dispersion in a generic urban neighborhood with multiple layouts of avenue-trees were studied. In a first step, a grid sensitivity study was performed that inferred that a cell count of 20 per building height and 12 per canyon width is sufficient for reasonable grid insensitive solutions. Next, the performance of the realizable k-ε turbulence model in simulating urban flows and of the applied vegetation model in simulating flow and turbulence in trees was validated. Finally, based on simulations of street canyons with and without avenue-trees, an appropriate turbulent Schmidt number for modeling dispersion in the urban neighborhood was determined as $Sc_t = 0.5$.

Capsule

Quality assessment and assurance studies were done for Computational Fluid Dynamics (CFD) simulations of the effects of avenue-trees on flow and dispersion in an urban neighborhood.

Keywords

CFD validation, built environment, pollutant dispersion, vegetation, turbulent Schmidt number

1. Introduction

The main purpose of this two-part study is to investigate how avenue-trees affect the natural ventilation and pollutant dispersion in a network of street canyons by means of Computational Fluid Dynamics (CFD) for a generic urban neighborhood. The study is motivated by recent research which showed that for isolated urban street canyons and street sections with trees generally increased traffic-emitted pollutant concentrations were found in comparison to their tree-free counterparts (Balczo et al., 2009; Buccolieri et al., 2011, 2009; Gromke, 2011; Gromke et al., 2008; Gromke and Ruck, 2012, 2009, 2007; Salim et al., 2011; Vos et al., 2013).

In this part, quality assessment and assurance studies prerequisite to reliable CFD simulations based on the Reynolds-averaged Navier Stokes (RANS) equations of flow and pollutant dispersion in a generic urban neighborhood including the aerodynamic effects of avenue-trees are presented. General guidelines and recommendations for evaluating and performing CFD simulations with respect to building aerodynamics and urban flows can be found e.g. in Blocken (2014), Blocken and Gualtieri (2012), Franke et al. (2007), Franke et al. (2011), Schatzmann and Leitl (2002), Schatzmann and Leitl (2009) and Tominaga et al. (2008). However, a sound approach requires also an individual consideration of the case at hand with a more specific evaluation in terms of quality assessment and assurance.

A crucial aspect for reliable CFD simulations is the grid resolution in the area of interest. The above mentioned guidelines and recommendations specify a minimum cell count of 10 per cube root of the building volume and per building separation. However, they also explicitly state that the actually required grid resolution is strongly problem dependent and no generally valid recommendation can be given in advance. Hence, grid sensitivity studies are needed for simulations of flow and transport phenomena in the urban environment. Typical required cell counts in CFD studies of flow, wind comfort, microclimate, natural ventilation or pollutant dispersion in street canyons or urban setups generally range from 8 to 32 cells per building height for low to medium high buildings and even more for high-rise buildings (e.g. Gromke et al., 2015; Janssen et al., 2013; Milliez and Carissimo, 2007; Montazeri et al., 2013; Moonen et al., 2013, 2012, 2011; Salim et al., 2011; Toparlar et al., 2015; Van Hooff and Blocken, 2010; Vos et al., 2013). The large span in cell counts underlines the requirement of a careful treatment of grid resolution issues and indicates future research demands.

Furthermore, of major importance in air quality studies is the specification of an appropriate turbulent Schmidt number Sc_t for dispersion modeling of near-ground emitted pollutants in a network of urban street canyons. The turbulent Schmidt number Sc_t is a fitting parameter, similar to the constants in turbulence models, which differs for different configurations. Former studies revealed a large variation in the appropriate turbulent Schmidt number for dispersion around isolated or grouped buildings and in street canyons (e.g. Blocken et al., 2008; Di Sabatino et al., 2008, 2007; Gousseau et al., 2011a, 2011b; Gromke et al., 2008; Li and Stathopoulos, 1997; Milliez and Carissimo, 2007; Tominaga and Stathopoulos, 2013, 2007; Wang and McNamara, 2006). Depending on source location and approach wind direction, turbulent Schmidt numbers Sc_t = 0.2 - 1.3 were found. In the present research, the situation is even more complicated since the urban neighborhood consists of intersections and street canyons with different orientations to the approach flow and with or without avenue-trees. Hence, a pre-study on an appropriate turbulent Schmidt number is crucial for reliable RANS CFD simulations.

In the remainder of Part I, Section 2 introduces the investigated generic urban neighborhood, the computational domain with its boundary conditions and other numerical settings. Comprehensive quality assessment and assurance studies are reported in Section 3. They comprise (i) a grid sensitivity study, (ii) a validation study for the Reynolds-averaged Navier Stokes equations (RANS) with realizable k-ε turbulence closure to simulate flows in a generic urban neighborhood and (iii) a validation study of the applied vegetation model to simulate mean flow and turbulence in trees. Section 4 presents an analysis

on the appropriate turbulent Schmidt number Sc_t for the generic urban neighborhood. Together, the set of quality assessment and assurance studies, and the analysis on the turbulent Schmidt number can be considered as a practical example with guideline character for consistent and integrated quality assessment and assurance in CFD. Summary and Conclusions are given in Section 5.

Part II (Gromke and Blocken, 2014) presents the concentration results for various layouts of avenue-trees and analyses their impact on flow and pollutant dispersion in an urban neighborhood.

2. Material and Methods

2.1 Urban Neighborhood and Computational Domain

A generic urban neighborhood consisting of 7 x 7 building blocks of 90 m x 90 m x 30 m (L x W x H) and corresponding street canyons of 90 m length, 18 m width and 30 m height was investigated (Fig. 1, top). Various scenarios differing in the avenue-tree layout were studied. The trees were always positioned horizontally centered in the street canyons with crowns of 6 m width and 12 m height, starting 6 m above the street level (Fig. 1, bottom). More details about the avenue-tree layouts are provided in Part II of this two-part contribution, see Gromke and Blocken (2014).

The computational domain size and boundary conditions were made such that the recommendations specified in Franke et al. (2007), Franke et al. (2011) and Tominaga et al. (2008) were fulfilled, see Fig. 1, top. Given the symmetric geometry and flow conditions, a symmetry boundary condition was assigned to the streamwise-central vertical plane, effectively modeling only half of the computational domain shown in Fig. 1, top. A symmetry boundary condition was assigned to the outer lateral side and the domain top, and a pressure outlet condition to the outflow boundary. At the inflow boundary, vertical profiles for mean velocity U (Eq. 1), turbulence kinetic energy k (Eq. 2), and turbulence dissipation rate ε (Eq. 3) for a neutrally stratified atmospheric boundary layer were imposed following Richards and Hoxey (1993) and Richards and Norris (2011) according to

$$U(z) = \frac{u_*}{\kappa} \ln\left(\frac{z + z_0}{z_0}\right) \tag{1}$$

$$k(z) = \frac{u_*^2}{\sqrt{c_\mu}} \tag{2}$$

$$\varepsilon(z) = \frac{u_*^3}{\kappa (z + z_0)} \tag{3}$$

with z the vertical position above ground, z_0 = 1.0 m the aerodynamic roughness length representative for urban terrain (Wieringa, 1992), κ = 0.40 the van Karman constant, u_* = 1.18 ms^{-1} the friction velocity and c_μ = 0.09. The resulting wind speed for the undisturbed approach flow at building height H = 30 m is U_H = 10 ms^{-1} and the Reynolds number based on H and U_H is $Re_H = 20x10^6$.

Based on a grid sensitivity study (Section 3.1), cubic cells with 1.5 m edge length were created to discretize the street canyons within the building array giving cell counts of 20 and 12 cells over the canyon height and width, respectively. Away from the building array, the grid was expanded by a stretching factor of 1.2 resulting in a structured grid with approximately 4.0 million hexahedral cells.

The building facades and roofs as well as the streets within the block array were modeled as flat surfaces with non-slip boundary conditions. In order to account for their actually rough surfaces, an aerodynamic roughness length $z_0 = 0.03$ m was assigned according to (Blocken and Persoon, 2009). The employed CFD code however requires a roughness specification in terms of equivalent sand grain roughness height k_s in combination with a roughness constant c_s. Moreover, k_s has to be smaller than half the wall-normal height of the wall adjacent cell. Applying the formula $k_s = 9.793\ z_0/c_s$ (Blocken et al., 2007a, 2007b) with $c_s = 7$ results in $k_s = 0.042$ m. The aerodynamic roughness length of the remaining ground surface was set $z_0 = 0.35$ m which translates with $c_s = 7$ into $k_s = 0.49$ m. Thus, the roughness heights comply with the requirement of being smaller than half the wall-normal cell height everywhere in the computational domain.

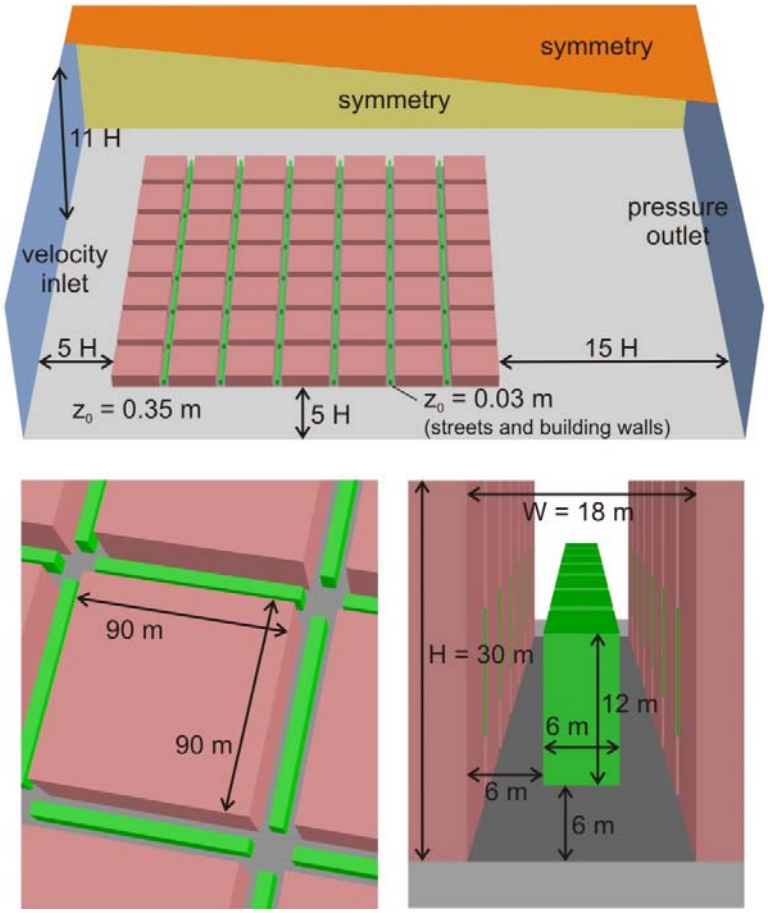

Fig. 1: Computational domain with urban neighborhood and avenue-trees. H = 30 m is the building height. Note that for the simulations a symmetry boundary condition was employed along the streamwise-central vertical plane.

2.2 Numerical Settings and Vegetation Model

The Computational Fluid Dynamics (CFD) code ANSYS FLUENT 12.4.1 (ANSYS, 2009a) was used to solve the steady state Reynolds-averaged Navier Stokes (RANS) equations closed by the realizable k-ε

turbulence model (Shih et al., 1995) with standard wall functions (Launder and Spalding, 1974) modified for roughness (Cebeci and Bradshaw, 1977).

The crowns of the trees were defined as porous fluid zones to which additional terms constituting the vegetation model were assigned. These additional terms accounted for the effects of vegetation on mean flow and turbulence following the formulation presented in Green (1992), Liu et al. (1996) and Sanz (2003). In particular, terms were added to the transport equations of momentum (Eq. 4), turbulence kinetic energy (Eq. 5) and turbulence dissipation rate (Eq. 6) at computational cells which contain vegetation according to

$$S_{U_i} = -\rho C_d \, LAD \, U_i \, \mathbf{U} \tag{4}$$

$$S_k = \rho C_d \, LAD \, (\beta_p \mathbf{U}^3 - \beta_d \mathbf{U} k) \tag{5}$$

$$S_\varepsilon = \rho C_d \, LAD \, \frac{\varepsilon}{k} (C_{\varepsilon 4} \beta_p \mathbf{U}^3 - C_{\varepsilon 5} \beta_d \mathbf{U} k) \, . \tag{6}$$

Notice that the extra terms in the transport equations of turbulence kinetic energy k and dissipation rate ε consist of both a source and sink contribution. This is to account for the enhanced production of turbulence, i.e. wake turbulence by short-circuiting the eddy cascade, which in turn due to its smaller length scales compared to shear turbulence is subjected to faster dissipation so that vegetation can act as a net sink for turbulence kinetic energy (e.g. Endalew et al., 2010, 2009; Green, 1992; Green et al., 1995; Mochida et al., 2008; Wilson and Shaw, 1977).

In Eqs. (4 - 6) ρ is the density of air, C_d the leaf drag coefficient, LAD the leaf area density, U_i the velocity component of direction i, **U** the velocity magnitude and k the turbulence kinetic energy. The leaf drag coefficient C_d depends on the species and in literature values ranging between 0.1 and 0.3 can be found where most commonly $C_d = 0.2$ is used. In this study $C_d = 0.2$ was set to reflect an average value instead of a species specific value. The leaf area density LAD also depends on the species and varies with height z over the tree crown. It typically assumes values between 0.5 and 2.0 m^2m^{-3} for deciduous trees. However, for practical purposes a constant, height-independent leaf area density of LAD = 1.0 m^2m^{-3} reflecting an average value, rather than a species specific value, was assigned. β_p and β_d are parameters with physical meaning where β_p is the fraction of mean kinetic energy that is converted into wake turbulence kinetic energy ($\beta_p = 0…1$) and β_d accounts for short-circuiting of the eddy cascade. $C_{\varepsilon 4}$ and $C_{\varepsilon 5}$ are empirical constants similar to the constants in turbulence models. Based on the analytical work of Sanz (2003) and the comprehensive flow simulations for various deciduous and coniferous forests by Katul et al. (2004), the parameters and coefficients were set to $\beta_p = 1.0$, $\beta_d = 5.1$ and $C_{\varepsilon 4} = C_{\varepsilon 5} = 0.9$.

For simulating traffic emissions, a passive (non-buoyant, non-reactive) scalar was released from the entire street surface within the building block array by specifying a constant flux boundary condition. Its dispersion was modeled by solving a steady state Reynolds-averaged advection-diffusion equation with the turbulent mass diffusivity derived from the momentum turbulent diffusivity (eddy diffusivity) and the turbulent Schmidt number Sc_t. Based on comparison of pollutant concentrations in street canyons with wind-tunnel measurements (Section 4), the dispersion simulations were performed with $Sc_t = 0.5$.

Second order discretizations were applied throughout and the SIMPLE scheme was used for pressure-velocity coupling. The CFD code default relaxation factors were applied (ANSYS, 2009a). The steady state simulations were iterated until the scaled residuals of all variables were either fallen below 10^{-8} or did not change anymore and the flow quantities at representative monitoring points within the computational domain assumed constant values.

3. Quality Assessment and Assurance Studies

Prior to the flow and pollutant concentration simulations in the urban neighborhood with avenue-trees, pre-studies for quality assessment and assurance were performed. They comprise a grid sensitivity study (Section 3.1), an assessment study of the employed realizable k-ε turbulence model for predicting flows in a generic urban neighborhood (Section 3.2), and an assessment study of the applied vegetation model for predicting flow through trees (Section 3.3).

3.1 Grid Sensitivity Study

To determine the required grid resolution, a grid sensitivity study was performed in the computational domain with the building block array (Fig. 1) by making use of the symmetry conditions. Four grids with cubical cells of 3.0, 2.0, 1.5 and 1.0 m inside the urban street canyons corresponding to cell counts of 10, 15, 20 and 30 along the building height H were generated. Outside the building block array an expansion ratio of 1.2 was applied to the cells resulting in final grids of 0.8, 1.8, 4.0 and 10.1 million hexahedral cells, respectively. The boundary conditions and the numerical settings were the same as detailed in Section 2.

The grid sensitivity study involved the comparison of the mean horizontal wind velocity U along vertical profiles at two locations with different flow regimes which were considered to be representative for the urban neighborhood. One profile was located in the center of an intersection (the intersection of the second wind-perpendicular street with the wind-parallel street directly next to the streamwise-central line); the other profile was located in the center of a wind-perpendicular street canyon (in the second wind-perpendicular street directly next to the streamwise-central building blocks).

As can be seen in Fig. 2, the profiles indicate some grid dependency which becomes smaller on the finer grids. For both locations, very little quantitative differences are present between the 1.5 m-grid and the 1.0 m-grid whereas for the 2.0 m-grid in comparison to the 1.5 m-grid even qualitative differences are found (bottom panel). This suggests the 1.5 m-grid with a cell count of 20 per building height and 12 per canyon width as appropriate for reliably predicting flows in the urban neighborhood. Note that these cell counts corroborate the best practice guidelines (Franke et al., 2011, 2007; Tominaga et al., 2008) who specify that 10 is a minimum cell count, suggesting indeed that higher numbers might be needed. Other CFD studies of flow and scalar transport in urban street canyons or urban setups of rather uniform height generally employed between 8 and 32 cell counts per building height (e.g. Balczo et al., 2009; Buccolieri et al., 2011, 2009; Gromke et al., 2015, 2008; Milliez and Carissimo, 2007; Moonen et al., 2013, 2012, 2011; Salim et al., 2011; Toparlar et al., 2015; Vos et al., 2013).

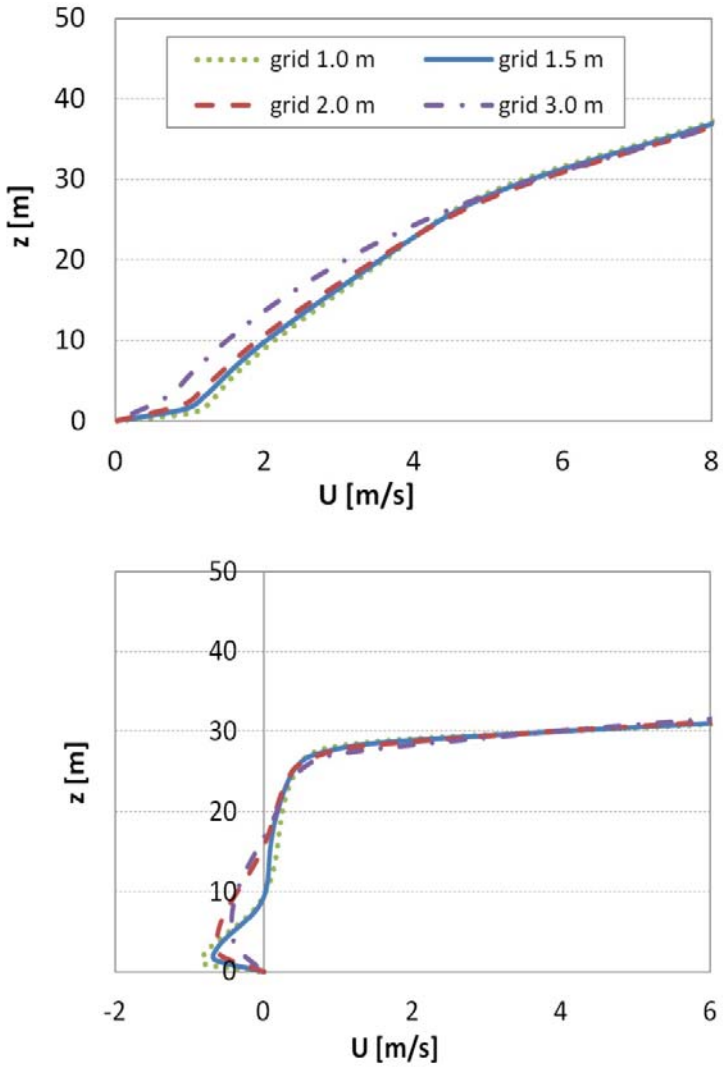

Fig. 2: Mean horizontal wind velocities U on different grids at the intersection (top) and wind-perpendicular (bottom) street canyon.

In order to obtain some quantitative metrics for the discretization error, the fractional error e_r according to

$$e_{r,i} = \frac{f_{2,i} - f_{1,i}}{f_{1,i}} \tag{7}$$

and the mean Grid Convergence Index (GCI) according to

$$GCI_i = \frac{\alpha \left| \left(f_{2,i} - f_{1,i} \right) / f_{1,i} \right| r_{21}^{p}}{r_{21}^{2} - 1} \tag{8}$$

as proposed in Roache (1997, 1994) have been estimated. The GCI is based on the generalized Richardson Extrapolation (Richardson, 1927) and aims at the uniform reporting of grid sensitivity study outcomes. In comparison to the generalized Richardson Extrapolation it provides a conservative estimate for the grid error. Here, $f_{2,i}$ is the solution on the 1.5 m-grid and $f_{1,i}$ the solution on the 1.0 m-grid at position i, r_{21} is the grid refinement ratio (r_{21} = 1.5 m/1.0 m = 1.5), p is the order of the method and α is a safety factor which is either 1.25 or 3.0 depending on how the order of the method p was estimated. Here, p was estimated by the transcendental equation, see Eq. (5) in Franke et al. (2007), according to

$$p_i = \frac{\ln\left[\left(f_{3,i} - f_{2,i}\right)/\left(f_{2,i} - f_{1,i}\right)\right]}{\ln(r_{21})} - \frac{1}{\ln(r_{21})}\left[\ln\left(r_{32}^{p_i} - 1\right) - \ln\left(r_{21}^{p_i} - 1\right)\right] \qquad (9)$$

at the intersection and α = 1.25, whereas at the center of the wind-perpendicular street canyon p was taken to the formal order of the method, i.e. p = 2, and α = 3.0 since the non-asymptotic behavior of the solutions on the 3 finest grids prevented a reliable estimation of the order p according to Eq. (9).

For the vertical profiles of velocity component U at the intersection and the center of the wind-perpendicular street canyon, average fractional errors e_r of 3.1 and 22.3%, respectively, related to the 1.0 m-grid were obtained. The corresponding average GCI values, related to the 1.5 m-grid, were determined to 10.1 and 120.4%. The percentage average fractional error and GCI value for the center of the wind-perpendicular street canyon appear rather large. However, they have to been seen in the light of the small flow velocities at this location (Fig. 2, bottom) and the large safety factor of α = 3.0.

3.2 Assessment Study of the realizable k-ε Turbulence Model

The next step of the quality assessment and assurance addresses the capability of the realizable k-ε turbulence model to simulate flows in generic urban configurations with grid characteristics mostly consistent and comparable to those obtained from the preceding grid sensitivity study (Section 3.1). To this end, CFD simulations of a 3 x 3 block array as available from the Architectural Institute of Japan (AIJ) database (AIJ Architectural Institute of Japan, Mochida et al., 2006; Mochida and Lun, 2008; Tominaga et al., 2008; Yoshie et al., 2007) were performed. The array consisted of 9 cubic blocks with 0.2 m edge length regularly spaced 0.2 m apart from each other (Fig. 3). In order to allow, as far as possible, for grid consistency and comparability, the street canyons within the block array were discretized by cubical cells of uniform size and the building height was resolved by a cell count of 20, resulting in cells with 0.01 m edge length which were expanded outside the block array by a stretching factor of 1.2. Due to the distinct geometry relative to the 7 x 7 generic neighborhood, inevitably not all edge-cell counts could be maintained and the those along the street width and building length were different. However, by the chosen approach, all principal directions were resolved equally fine without favoring one over the other. Moreover, maintaining all edge-cell counts would have resulted in cells within the street canyons with unfavorable grid quality metrics.

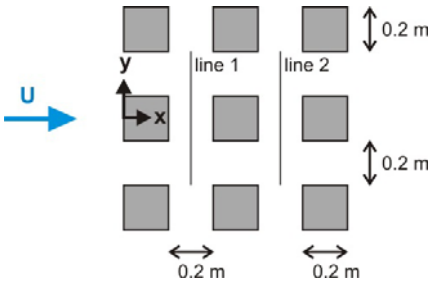

Fig. 3: Ground plan of cubic block array employed in the wind tunnel measurements (AIJ Architectural Institute of Japan).

The computational domain was made to mimic the wind tunnel dimensions and boundary conditions with smooth walls at the lateral and top sides and velocity inlet and pressure outlet boundary condition at the streamwise-normal inflow and outflow sides, respectively. To the ground surface and the block walls different roughnesses were assigned as will be specified later. The distance from the inlet to the windward side of the first block row was 5 H and from the leeward side of the last block row to the outlet was 15 H complying with the recommendations in guidelines (Franke et al., 2011, 2007; Tominaga et al., 2008). At the inlet a velocity profile U(z) and a turbulence kinetic energy profile k(z) based on provided wind tunnel data were imposed whereby the turbulence kinetic energy was derived from the streamwise fluctuating velocity component u' according to the following formula

$$k(z) = \frac{1}{2}\overline{u_i' u_i'} \cong \frac{1}{2}\left(\overline{u'u'} + \left(\frac{1.9}{2.5}\right)^2 \overline{u'u'} + \left(\frac{1.3}{2.5}\right)^2 \overline{u'u'}\right) = \frac{1}{2}\left(1.85\ \overline{u'u'}\right) \qquad (10)$$

with u_i' the fluctuating part of the i^{th} velocity component. The pre-factors are based on observations in neutrally stratified surface layers (e.g. Stull, 1988). For the dissipation rate ε(z) a hyperbolic profile according to Eq. 3 with $u_* = 0.35\ ms^{-1}$ and $z_0 = 0.0018$ m was imposed whereby u_* and z_0 were determined by fitting the logarithmic velocity profile (Eq. 1) to the provided measured velocity data. The imposed profiles of velocity U(z), turbulence kinetic energy k(z) and dissipation rate ε(z) are shown in Fig. 4.

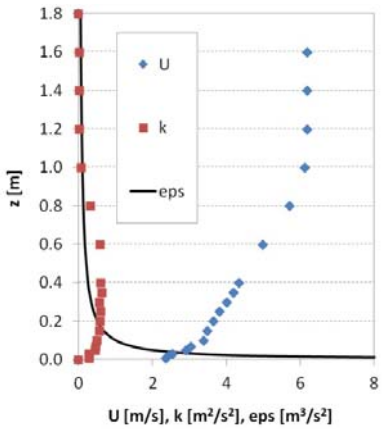

Fig. 4: Inlet profiles of velocity U(z), turbulence kinetic energy k(z) and dissipation rate ε(z).

The ground and block surfaces roughnesses in the wind tunnel experiment were classified as “smooth” (AIJ Architectural Institute of Japan) leaving their actual aerodynamic roughness lengths unspecified. To this end, CFD simulations with different ground and block surface roughness lengths were performed allowing to assess their impact. Simulations with nine pairs of ground and block surface roughness lengths were performed with values for $z_{0,ground}$ = 0 - 0.0011 m and $z_{0,block}$ = 0 - 0.0018 m which, for a roughness constant c_s = 7, correspond to roughness heights $k_{s,ground}$ = 0 - 0.0015 m and $k_{s,block}$ = 0 - 0.0025 m (Blocken et al., 2007a, 2007b), hence being always smaller than half the wall-normal cell height (0.005 m). The remaining numerical settings were the same as for the urban neighborhood consisting of 7 x7 building block array (Section 2).

Fig. 5 compares wind speed measurements from the wind tunnel obtained by non-directional thermistor anemometry with CFD simulations for four pairs of ground and block surface roughness lengths. The magnitude of the wind speed **U** was measured at 0.02 m above ground along two lines, see Fig. 3, and was normalized by the approach flow velocity $U_{0.02,approach}$ at 0.02 m height. It is noted that the CFD results were modified according to $\mathbf{U}_{mod} = (\mathbf{U}^2_{CFD} + 2 \cdot k)^{1/2}$ for the comparison with the thermistor anemometry data (Tominaga et al., 2005).

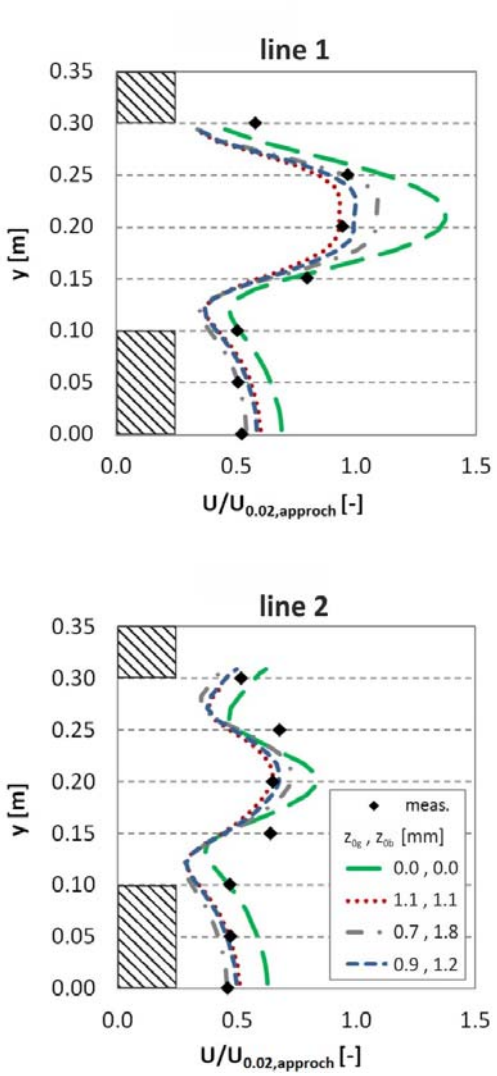

Fig. 5: Comparison of measured and simulated wind speeds at 0.02 m above ground for different ground and block roughness lengths, z_{0g} and z_{0b}, respectively. The hatched rectangles indicate the positions of the building blocks.

As can be seen from Fig. 5, the CFD simulations qualitatively predict the near-ground wind speed pattern along line 1 and line 2 in the block array with smaller wind speeds in the lee of the blocks and larger wind speeds in the passages. The results show a substantial sensitivity of the near-ground wind speed on the ground and block surface roughness lengths. The simulations with zero roughness lengths resulted in general in too high wind speeds relative to the measurements. Assigning non-zero roughness lengths to the ground and block surfaces resulted in reduced simulated wind speeds in closer agreement with the measurement data. Average deviations ranging from 13.4% underestimation to 8.1% overestimation were obtained in the simulations with different wall roughness lengths. Based on these acceptable deviations, it is concluded that the realizable k-ε turbulence model is capable of reliably simulating flows in the generic urban neighborhood for the given grid characteristics.

3.3 Assessment Study of the Vegetation Model

For the validation of the vegetation model (Eq. 4-6), field measurement data from Amiro (1990) in a 12 m high aspen forest were employed. The equations for modeling the effects of vegetation on mean flow and turbulence were implemented as User-Defined-Functions (UDF) in the computational simulations (ANSYS, 2009b). A computational domain with dimensions of 30 m x 10 m x 500 m (L x W x H) was made and equipped with coupled periodic boundary conditions at the inflow and outflow side, a wall with zero-roughness at the ground, and symmetry boundaries at the lateral sides and top to mimic the developed flow in an extended forest (Fig. 6). The lower 12 m of the domain were defined as a porous fluid zone representing the aspen forest to which the leaf area density profile LAD(z) in place was assigned (Fig. 6). The forest stand was discretized by cubic cells of 1 m edge length, providing a grid resolution comparable to the one employed in the street canyons of the neighborhood (Section 2). Above the forest, the grid was expanded in vertical direction by a factor 1.2. An air mass flow rate of 40,000 kgs^{-1} was assigned at the inflow side, resulting in a streamwise wind velocity U = 2.6 ms^{-1} at 13.1 m height in the converged solution which is in close agreement with the field data of Amiro (1990) where a streamwise wind speed U = 2.3 ms^{-1} at the same height was measured. The other numerical settings including the set of values for the vegetation parameters and coefficients were the same as for the urban neighborhood simulations described in Section 2.

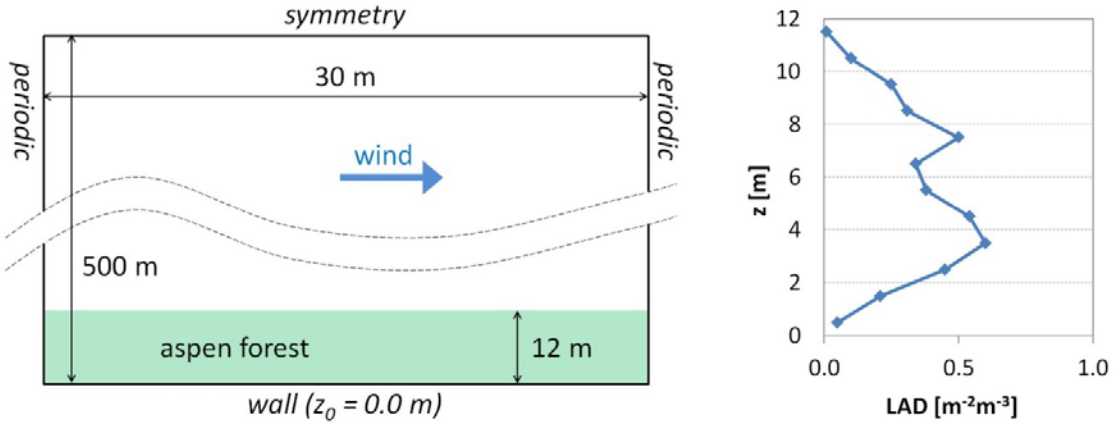

Fig. 6: Computational domain of the aspen forest and leaf area density LAD(z) profile.

Fig. 7 shows the simulation results together with the measurement data for the mean streamwise velocity U and the kinematic Reynolds stress <u'w'>. Following Amiro (1990), the results were normalized by the wind speed U_{ref} and the kinematic Reynolds stress $\langle u'w' \rangle_{ref}$ at 12 m height, and the height z above ground by the reference height h_{ref} = 10 m. In the case of mean streamwise velocity, the maximum relative difference between measurements and simulations is 27% and occurs at z/h_{ref} = 0.14. However, since the wind speed at this height is very small (~ 0.2 ms^{-1}), the difference in absolute velocities is very small, too. For the upper part of the aspen forest (z/h_{ref} > 0.5), a good agreement with relative differences smaller than 10% is found. On average, the numerical simulations slightly underestimate the measured mean streamwise velocity by 4.0%. With regard to the kinematic Reynolds stress <u'w'>, the CFD simulation in general underestimates the measurement data. The largest differences are present in the upper part of the forest canopy with a maximum relative difference of 43% at z/h_{ref} = 0.87. However, the measurement data in this part also show a large variability as indicated by the error bars. For the lower part of the canopy, a close agreement between both data sets is present. On average, the simulations underestimate the measured kinematic Reynolds stress by 34.9%

and the friction velocity $u_* = \langle u'w' \rangle^{0.5}$ by 25.0%. Overall, the comparison shows that the simulation with the implemented vegetation terms (Eq. 4-6) and the set of values for the vegetation parameters described in Section 2.2 are able to model the characteristics of the mean flow and shear stress profiles within the aspen forest. Hence, it is concluded that the vegetation model reliably simulates flow through vegetation by the employed grid resolution.

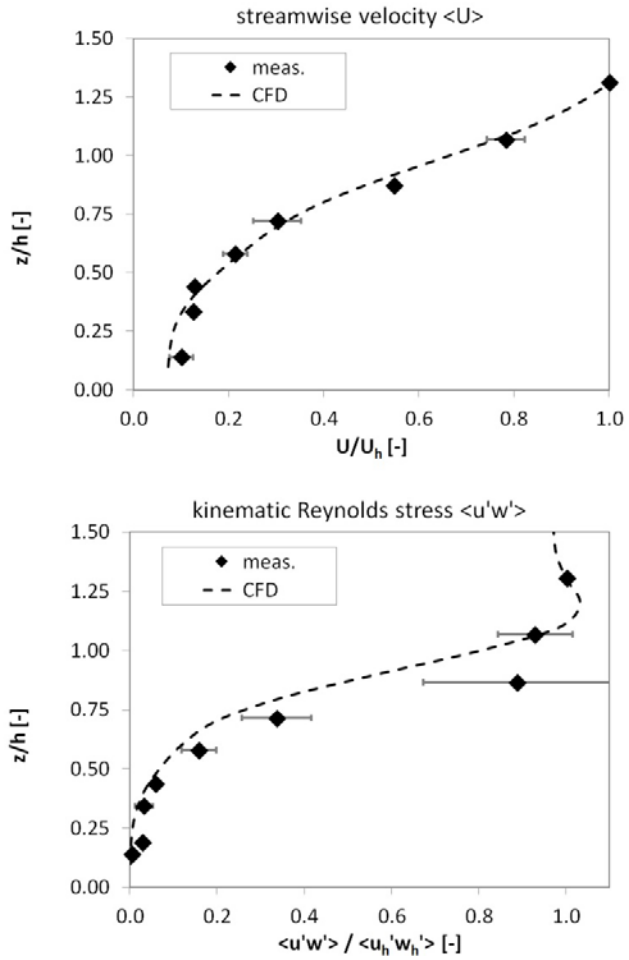

Fig. 7: Normalized streamwise velocity and normalized kinematic Reynolds stress. Error bars indicate ± 1 standard deviation.

4. Turbulent Schmidt Number Analysis

The turbulent Schmidt number Sc_t in a given flow field is spatially variable. It is a fitting parameter which depends on the mean and turbulent characteristics of a flow, on the position(s) and type(s) of the pollutant source(s) as well as on the abundance and the heterogeneity of the distribution of the pollutant species in space (e.g. Blocken et al., 2008; Koeltzsch, 2000; Tominaga and Stathopoulos, 2013, 2007). Studies on pollutant dispersion around isolated buildings and in the urban environment using classical turbulence closure schemes for RANS equations suggest values for Sc_t ranging from 0.2 to 1.3 (e.g. Blocken et al., 2008; Buccolieri et al., 2009; Di Sabatino et al., 2007; Gousseau et al., 2011a, 2011b; Gromke et al., 2008; Tominaga and Stathopoulos, 2013, 2007). This variability indicates the need for

careful considerations about the appropriate Sc_t number for each single study case. To this end, pollutant dispersion in urban street canyons with and without avenue-trees was simulated with different values for Sc_t and validated against wind tunnel data from the internet data base CODASC - Concentration Data of Street Canyons (CODASC, 2008; Gromke and Ruck, 2012).

Fig. 8 shows the isolated urban street canyon for which CFD simulations with perpendicular and parallel approach flow were performed. The model buildings have a height H = 0.12 m, a length of L = 1.2 m and the street canyon width is W = 0.12 m. The computational domain was made in agreement with the wind tunnel setup. Zero-roughness wall boundary conditions were applied to the top, the lateral sides as well as to the building models and the street in-between them. A roughness length $z_0 = 0.0021$ m, corresponding to a roughness height $k_s = 0.003$ m with $c_s = 7$ (Blocken et al., 2007a, 2007b), was assigned to the ground. The tree crowns were modeled as porous media with pressure loss coefficient $\lambda = 80\ m^{-1}$ according to Gromke (2011) and Gromke and Ruck (2012) in which the terms for vegetation-affected transport of momentum (Eq. 4), turbulence kinetic energy (Eq. 5) and turbulence dissipation rate (Eq. 6) were enabled where $\lambda = C_d \cdot LAD$. The distances between the inlet and outlet boundaries to the outermost building faces complied with the guidelines of Franke et al. (2011, 2007) and Tominaga et al. (2008). At the inflow side a power-law velocity profile as measured in the wind tunnel according to

$$U(z) = U_{ref}\left(\frac{z}{z_{ref}}\right)^{\alpha} \tag{11}$$

with $\alpha = 0.30$, $z_{ref} = 0.12$ m and $U_{ref} = 4.70\ ms^{-1}$ and profiles for turbulence kinetic energy k and dissipation rate ε according to Eq. (2) and Eq. (3), respectively, with $u_* = 0.52\ ms^{-1}$ and $z_0 = 0.0037$ m were applied. The outflow side was specified as pressure outlet boundary condition. Inside the street canyon and adjacent to the buildings, hexahedral cells (cuboids) of height $c_h = H/18$ with length and width $c_l = c_w = H/12$, providing a similar cell count as in the neighborhood building block array (section 2), were employed which were expanded by a factor of 1.2 outside. Hence, the condition of the roughness height $k_s = 0.003$ m being smaller than half the wall-normal cell height (0.0033 m) was fulfilled everywhere in the computational domain. To mimic the emission source characteristics of the experiments, the wind tunnel line sources were represented by elongated areas at the ground level from which a specified mass flux of tracer gas (sulfur hexafluoride) was released. More details about the wind tunnel line source characteristics can be found in the internet data base CODASC - Concentration Data of Street Canyons (CODASC, 2008). The tracer gas was treated as a passive, non-reactive scalar in the dispersion simulations and the remaining numerical settings were the same as those described in Section 2 for the neighborhood simulations.

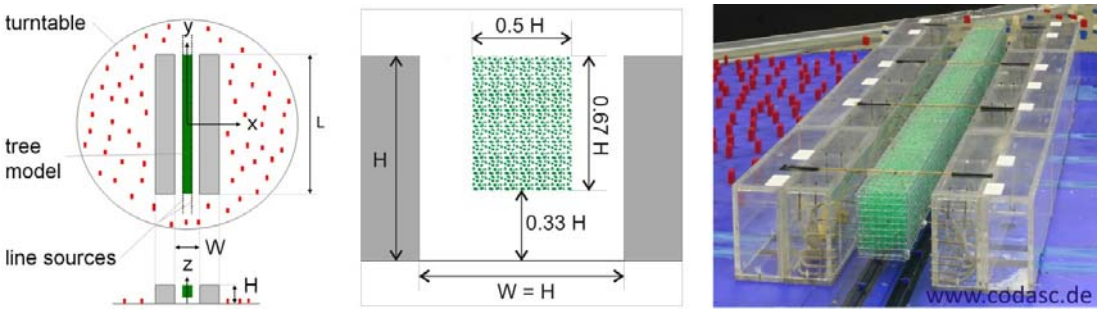

Fig. 8: Isolated urban street canyon model with avenue-tree row (CODASC, 2008).

Fig. 9 presents concentrations at the building walls facing the street canyon obtained by CFD simulations with $Sc_t = 0.3$, 0.5 and 0.7 in comparison to wind tunnel data for four configurations (perpendicular/parallel wind and with/without trees). The simulated and measured concentrations are given in normalized form, c^+_{sim} and c^+_{meas}, respectively, according to

$$c^+ = \frac{c\, U_{ref}\, H}{Q/l} \tag{12}$$

with c either the simulated or measured concentration, U_{ref} the approach flow velocity at building height H, Q the emission rate and l the line source length.

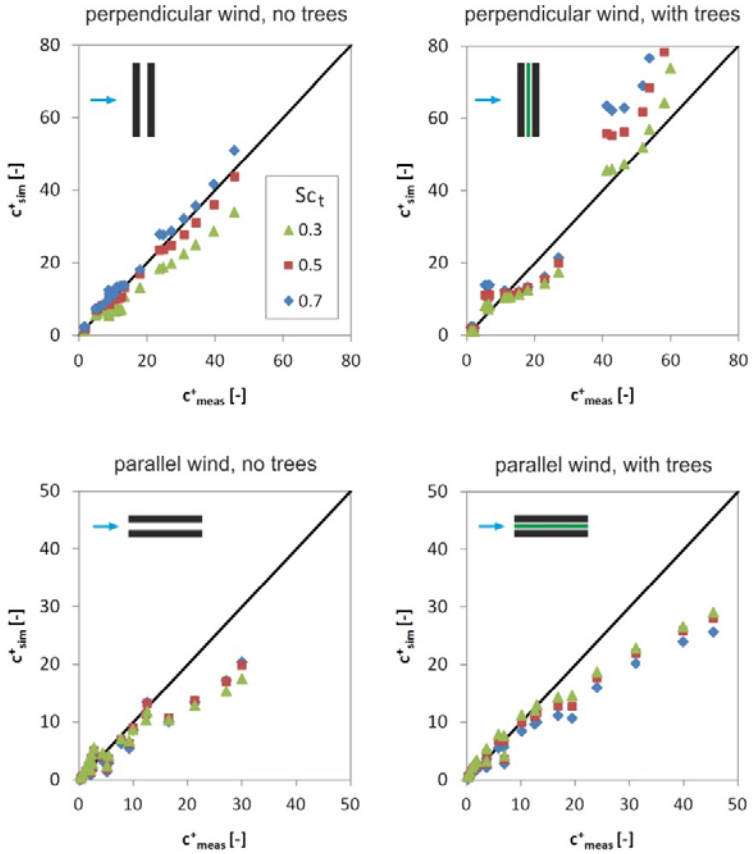

Fig. 9: Comparison of normalized concentrations at the building walls facing the street canyon from wind tunnel experiments c^+_{meas} and CFD simulations c^+_{sim} with different Sc_t. The concentration data were obtained from sampling sites distributed over the entire building walls.

Fig. 9 clearly shows that there is no single appropriate Sc_t, neither for all configurations nor within a certain configuration. The agreement between measured and simulated concentrations is better for perpendicular approach flow. For the higher concentrations, the simulations mostly overestimate the measurement data in the case of perpendicular approach flow whereas they underestimate them in the case of parallel approach flow. Lower Sc_t numbers result in general in decreased concentrations for

perpendicular wind but in increased concentrations for parallel wind. This is due to the relative position of the emission sources, i.e. the line sources at the street, to the sampling sites at the building facades and the prevailing flow field inside the canyon (Fig. 8). For perpendicular wind the effect of enhanced air exchange between the street canyon and the above roof level due to increased turbulent mixing results in lower concentrations at the building walls. For parallel wind the effect of increased lateral spreading yields amplified transport of pollutants from the line sources close the street center to the building facades. Fig. 9 indicates overall lower Sc_t numbers for parallel compared to perpendicular approach flow. In particular for the highest concentrations in the canyon with avenue-trees subjected to parallel wind, very low values for Sc_t are implied. Moreover, the upper two panels in Fig. 9 suggest different Sc_t for the canyon with and without trees.

In order to determine a single appropriate value of Sc_t for the pollutant dispersion simulations in the urban neighborhood (Fig. 1), four different metrics were applied (Eq. 13-16). Those were the normalized sum of the differences (NSD) according to

$$NSD = \frac{\sum_{i}^{N}\left(c^{+}_{i,sim} - c^{+}_{i,meas}\right)}{\sum_{i}^{N} c^{+}_{i,meas}} \tag{13}$$

with N the total number of concentration sampling points i, the normalized sum of the absolute differences (NSAD) according to

$$NSAD = \frac{\sum_{i}^{N}\left|c^{+}_{i,sim} - c^{+}_{i,meas}\right|}{\sum_{i}^{N} c^{+}_{i,meas}}, \tag{14}$$

the mean difference (MD) according to

$$MD = \frac{\sum_{i}^{N}\left(c^{+}_{i,sim} - c^{+}_{i,meas}\right)}{N} \tag{15}$$

and the mean absolute difference (MAD) according to

$$MAD = \frac{\sum_{i}^{N}\left|c^{+}_{i,sim} - c^{+}_{i,meas}\right|}{N} \tag{16}$$

The different metrics were calculated for each of the four configurations, i.e. for the street canyon with and without trees being subjected to perpendicular and parallel wind. Table 1 contains the mean values obtained by averaging over all configurations.

Table 1 Mean metrics obtained by averaging over all four configurations.

Sc_t	NSD	NSAD	MD	MAD
0.7	-0.3	32.1	1.0	4.4
0.5	-4.7	25.1	0.1	3.3
0.3	-13.5	25.5	-1.4	3.1

Since in the urban street canyon dispersion simulations the minima of the absolute values for two out of four mean metrics were obtained with a $Sc_t = 0.5$, it was decided to perform the dispersion simulations in the urban neighborhood with $Sc_t = 0.5$.

In addition to the herein followed approach of modeling the wind tunnel line sources by specifying constant flux boundary conditions at the discharge positions at the street surface, a CFD simulation with volume sources occupying the lowermost computational cells next to the ground was done for the tree-free canyon subjected to perpendicular wind. This source modeling approach was also followed in Gromke et al. (2008), Balczo et al. (2009) and Buccolieri et al. (2009) and was performed here in order to check the sensitivity of the dispersion simulations and appropriate Sc_t number on the type of source modeling. However, the concentrations showed only small deviations of 1% on average and 2% at maximum, hence indicating that the dispersion simulations and appropriate Sc_t number for the studied geometry are only marginally dependent on the type of source modeling.

5. Summary and Conclusions

Comprehensive quality assessment and assurance studies and a turbulent Schmidt number analysis for Computational Fluid Dynamics (CFD) simulations of flow and pollutant dispersion at the urban neighborhood scale including avenue-trees were performed. Four aspects relevant for reliable numerical microscale flow and dispersion modeling in the built environment were addressed, namely

- the required grid resolution was determined in a grid sensitivity study (Section 3.1)
- the ability of the Reynolds-averaged Navier Stokes (RANS) equations with realizable k-ε turbulence closure to predict flows in a generic urban neighborhood was investigated and the impact of different wall roughness lengths was checked (Section 3.2)
- the performance of the vegetation model to simulate mean flow and turbulence in trees was investigated (Section 3.3)
- an appropriate turbulent Schmidt number Sc_t for dispersion modeling in a generic urban neighborhood with and without avenue-trees was determined (Section 4).

Simulations on four computational grids were performed for the urban neighborhood. It was found that in the building canopy layer a grid count of 20 cells per building height and 12 cells per street width were sufficient for solutions with acceptable low grid sensitivity where the fractional error e_r and the Grid Convergence Index GCI were used to quantify the discretization error. The corresponding grid consisted of cubical cells with edge length of 1.5 m. The RANS equations with realizable k-ε turbulence closure to model urban flows were validated against wind tunnel data of velocities in a regular block array. Different wall roughness lengths of the surfaces within the block array were tested and their implications on the flow velocities were studied. A qualitative and reasonable quantitative agreement was obtained with average deviations ranging from 13.4% underestimation to 8.1% overestimation for the different wall roughness setups. The vegetation model for simulating flow and turbulence in trees was validated against full scale measurements in a forest. Close agreement was obtained for the mean streamwise velocity with a slight underestimation of 4.0% in average and moderate agreement for the friction velocity with an underestimation of 25.0% in average. The dispersion simulations for an urban

street canyon revealed a variability of the appropriate turbulent Schmidt number between the configurations with and without avenue-trees as well as for the conditions of perpendicular and parallel approach flow. This is even true for a single configuration, where the appropriate turbulent Schmidt number depends on the position within the canyon. However, based on various metrics, the appropriate turbulent Schmidt number for numerical modeling of pollutant dispersion in the generic urban neighborhood was estimated to $Sc_t = 0.5$. The concentrations and hence the appropriate turbulent Schmidt number were only negligibly sensitive to the type of emission source modeling (area versus volume source) with deviations in concentrations of 1% in average.

The quality assessment and assurance studies concerning the RANS CFD modeling of flows in the generic urban neighborhood, of mean flow and turbulence in vegetation canopies and the appropriate turbulent Schmidt number analysis were performed on computational grids with cells of comparable size or cell counts as determined in the grid sensitivity study, i.e. with either cubical cells of approximate edge length of 1.5 m or cell counts of approximate 20 cells per object edge. The comprehensive quality assessment and assurance studies with consistent grid resolution or cell count are considered to ensure meaningful CFD simulations of flow and pollutant dispersion in our study case of an urban neighborhood with various layouts of avenue-trees, see Part II (Gromke and Blocken, 2014).

Acknowledgements

Christof Gromke was supported by a Marie Curie Intra European Fellowship within the 7th European Community Framework Programme. The authors would like to thank Yoshihide Tominaga from Niigata Institute of Technology, Japan for kindly providing information as to the Architectural Institute of Japan (AIJ) database (AIJ Architectural Institute of Japan).

References

AIJ Architectural Institute of Japan, n.d. Guidebook for Practical Applications of CFD to Pedestrian Wind Environment around Buildings. doi:http://www.aij.or.jp/jpn/publish/cfdguide/index_e.htm

Amiro, B.D., 1990. Comparison of turbulence statistics within three boreal forest canopies. Bound.-Layer Meteorol. 51, 99–121.

ANSYS, 2009a. Ansys Fluent 12.0 Manual. ANSYS Inc.

ANSYS, 2009b. Ansys Fluent 12.0 UDF Manual. ANSYS Inc.

Balczo, M., Gromke, C., Ruck, B., 2009. Numerical modeling of flow and pollutant dispersion in street canyons with tree planting. Meteorol. Z. 18, 197–206.

Blocken, B., 2014. 50 years of Computational Wind Engineering: Past, present and future. J. Wind Eng. Ind. Aerodyn. 129, 69–102.

Blocken, B., Carmeliet, J., Stathopoulos, T., 2007a. CFD evaluation of wind speed conditions in passages between parallel buildings—effect of wall-function roughness modifications for the atmospheric boundary layer flow. J. Wind Eng. Ind. Aerodyn. 95, 941–962.

Blocken, B., Gualtieri, C., 2012. Ten iterative steps for model development and evaluation applied to Computational Fluid Dynamics for Environmental Fluid Mechanics. Environ. Model. Softw. 33, 1–22.

Blocken, B., Persoon, J., 2009. Pedestrian wind comfort around a large football stadium in an urban environment: CFD simulation, validation and application of the new Dutch wind nuisance standard. J. Wind Eng. Ind. Aerodyn. 97, 255–270.

Blocken, B., Stathopoulos, T., Carmeliet, J., 2007b. CFD simulation of the atmospheric boundary layer: wall function problems. Atmos. Environ. 41, 238–252.
Blocken, B., Stathopoulos, T., Saathoff, P., Wang, X., 2008. Numerical evaluation of pollutant dispersion in the built environment: comparisons between models and experiments. J. Wind Eng. Ind. Aerodyn. 96, 1817–1831.
Buccolieri, R., Gromke, C., Di Sabatino, S., Ruck, B., 2009. Aerodynamic effects of trees on pollutant concentration in street canyons. Sci. Total Environ. 407, 5247–5256.
Buccolieri, R., Salim, S.M., Leo, L.S., Di Sabatino, S., Chan, A., Ielpo, P., de Gennaro, G., Gromke, C., 2011. Analysis of local scale tree–atmosphere interaction on pollutant concentration in idealized street canyons and application to a real urban junction. Atmos. Environ. 45, 1702–1713.
Cebeci, T., Bradshaw, P., 1977. Momentum transfer in boundary layers. Wash. DC Hemisphere Publ. Corp N. Y. McGraw-Hill Book Co 1977 407 P 1.
CODASC, 2008. Concentration Data of Street Canyons. doi:www.codasc.de
Di Sabatino, S., Buccolieri, R., Pulvirenti, B., Britter, R., 2007. Simulations of pollutant dispersion within idealised urban-type geometries with CFD and integral models. Atmos. Environ. 41, 8316–8329.
Di Sabatino, S., Buccolieri, R., Pulvirenti, B., Britter, R.E., 2008. Flow and pollutant dispersion in street canyons using FLUENT and ADMS-Urban. Environ. Model. Assess. 13, 369–381.
Endalew, A.M., Debaer, C., Rutten, N., Vercammen, J., Delele, M.A., Ramon, H., Nicolaï, B.M., Verboven, P., 2010. A new integrated CFD modelling approach towards air-assisted orchard spraying. Part I. Model development and effect of wind speed and direction on sprayer airflow. Comput. Electron. Agric. 71, 128–136.
Endalew, A.M., Hertog, M., Gebrehiwot, M.G., Baelmans, M., Ramon, H., Nicolaï, B.M., Verboven, P., 2009. Modelling airflow within model plant canopies using an integrated approach. Comput. Electron. Agric. 66, 9–24.
Franke, J., Hellsten, A., Schlünzen, H., Carissimo, B., 2007. Best practice guideline for the CFD simulation of flows in the urban environment, in: COST Action. p. 51.
Franke, J., Hellsten, A., Schlunzen, K.H., Carissimo, B., 2011. The COST 732 Best Practice Guideline for CFD simulation of flows in the urban environment: a summary. Int. J. Environ. Pollut. 44, 419–427.
Gousseau, P., Blocken, B., Stathopoulos, T., Van Heijst, G.J.F., 2011a. CFD simulation of near-field pollutant dispersion on a high-resolution grid: a case study by LES and RANS for a building group in downtown Montreal. Atmos. Environ. 45, 428–438.
Gousseau, P., Blocken, B., Van Heijst, G.J.F., 2011b. CFD simulation of pollutant dispersion around isolated buildings: On the role of convective and turbulent mass fluxes in the prediction accuracy. J. Hazard. Mater. 194, 422–434.
Green, S.R., 1992. Modelling turbulent air flow in a stand of widely-spaced trees. Phoenics J 5, 294–312.
Green, S.R., Grace, J., Hutchings, N.J., 1995. Observations of turbulent air flow in three stands of widely spaced Sitka spruce. Agric. For. Meteorol. 74, 205–225.
Gromke, C., 2011. A vegetation modeling concept for Building and Environmental Aerodynamics wind tunnel tests and its application in pollutant dispersion studies. Environ. Pollut. 159, 2094–2099.
Gromke, C., Blocken, B., 2014. Influence of avenue-trees on air quality at the urban neighborhood scale. Part II: Traffic pollutant concentrations at pedestrian level, submitted to Environmental Pollution.
Gromke, C., Blocken, B., Janssen, W., Merema, B., van Hooff, T., Timmermans, H., 2015. CFD analysis of transpirational cooling by vegetation: Case study for specific meteorological conditions during a heat wave in Arnhem, Netherlands. Build. Environ., http://dx.doi.org/10.1016/j.buildenv.2014.04.022.

Gromke, C., Buccolieri, R., Di Sabatino, S., Ruck, B., 2008. Dispersion study in a street canyon with tree planting by means of wind tunnel and numerical investigations–evaluation of CFD data with experimental data. Atmos. Environ. 42, 8640–8650.
Gromke, C., Ruck, B., 2007. Influence of trees on the dispersion of pollutants in an urban street canyon—experimental investigation of the flow and concentration field. Atmos. Environ. 41, 3287–3302.
Gromke, C., Ruck, B., 2009. On the impact of trees on dispersion processes of traffic emissions in street canyons. Bound.-Layer Meteorol. 131, 19–34.
Gromke, C., Ruck, B., 2012. Pollutant concentrations in street canyons of different aspect ratio with avenues of trees for various wind directions. Bound.-Layer Meteorol. 144, 41–64.
Janssen, W.D., Blocken, B., van Hooff, T., 2013. Pedestrian wind comfort around buildings: Comparison of wind comfort criteria based on whole-flow field data for a complex case study. Build. Environ. 59, 547–562.
Katul, G.G., Mahrt, L., Poggi, D., Sanz, C., 2004. One-and two-equation models for canopy turbulence. Bound.-Layer Meteorol. 113, 81–109.
Koeltzsch, K., 2000. The height dependence of the turbulent Schmidt number within the boundary layer. Atmos. Environ. 34, 1147–1151.
Launder, B.E., Spalding, D.B., 1974. The numerical computation of turbulent flows. Comput. Methods Appl. Mech. Eng. 3, 269–289.
Liu, J., Chen, J.M., Black, T.A., Novak, M.D., 1996. E-ε modelling of turbulent air flow downwind of a model forest edge. Bound.-Layer Meteorol. 77, 21–44.
Li, Y., Stathopoulos, T., 1997. Numerical evaluation of wind-induced dispersion of pollutants around a building. J. Wind Eng. Ind. Aerodyn. 67, 757–766.
Milliez, M., Carissimo, B., 2007. Numerical simulations of pollutant dispersion in an idealized urban area, for different meteorological conditions. Bound.-Layer Meteorol. 122, 321–342.
Mochida, A., Lun, I.Y., 2008. Prediction of wind environment and thermal comfort at pedestrian level in urban area. J. Wind Eng. Ind. Aerodyn. 96, 1498–1527.
Mochida, A., Tabata, Y., Iwata, T., Yoshino, H., 2008. Examining tree canopy models for CFD prediction of wind environment at pedestrian level. J. Wind Eng. Ind. Aerodyn. 96, 1667–1677.
Mochida, A., Tominaga, Y., Yoshie, R., 2006. AIJ guideline for practical applications of CFD to wind environment around buildings, in: 4th International Symposium on Computational Wind Engineering (CWE2006).
Montazeri, H., Blocken, B., Janssen, W.D., van Hooff, T., 2013. CFD evaluation of new second-skin facade concept for wind comfort on building balconies: Case study for the Park Tower in Antwerp. Build. Environ. 68, 179–192.
Moonen, P., Dorer, V., Carmeliet, J., 2011. Evaluation of the ventilation potential of courtyards and urban street canyons using RANS and LES. J. Wind Eng. Ind. Aerodyn. 99, 414–423.
Moonen, P., Dorer, V., Carmeliet, J., 2012. Effect of flow unsteadiness on the mean wind flow pattern in an idealized urban environment. J. Wind Eng. Ind. Aerodyn. 104, 389–396.
Moonen, P., Gromke, C., Dorer, V., 2013. Performance assessment of Large Eddy Simulation (LES) for modeling dispersion in an urban street canyon with tree planting. Atmos. Environ.
Richardson, L.F., 1927. The deferred approach to the limit. Philos. Trans. R. Soc. Lond. Ser. A 226, 299–361.
Richards, P.J., Hoxey, R.P., 1993. Appropriate boundary conditions for computational wind engineering models using the k-ϵ turbulence model. J. Wind Eng. Ind. Aerodyn. 46, 145–153.
Richards, P.J., Norris, S.E., 2011. Appropriate boundary conditions for computational wind engineering models revisited. J. Wind Eng. Ind. Aerodyn. 99, 257–266.
Roache, P.J., 1994. Perspective: a method for uniform reporting of grid refinement studies. J. Fluids Eng. 116, 405–413.

Roache, P.J., 1997. Quantification of uncertainty in computational fluid dynamics. Annu. Rev. Fluid Mech. 29, 123–160.
Salim, S.M., Cheah, S.C., Chan, A., 2011. Numerical simulation of dispersion in urban street canyons with avenue-like tree plantings: Comparison between RANS and LES. Build. Environ. 46, 1735–1746.
Sanz, C., 2003. A note on k-ε modelling of vegetation canopy air-flows. Bound.-Layer Meteorol. 108, 191–197.
Schatzmann, M., Leitl, B., 2002. Validation and application of obstacle-resolving urban dispersion models. Atmos. Environ. 36, 4811–4821.
Schatzmann, M., Leitl, B., 2009. Evaluation of numerical flow and dispersion models for applications in industrial and urban areas. Chem. Eng. Technol. 32, 241–246.
Shih, T.-H., Liou, W.W., Shabbir, A., Yang, Z., Zhu, J., 1995. A new k-ϵ eddy viscosity model for high reynolds number turbulent flows. Comput. Fluids 24, 227–238.
Stull, R.B., 1988. An introduction to boundary layer meteorology. Springer.
Tominaga, Y., Mochida, A., Yoshie, R., Kataoka, H., Nozu, T., Yoshikawa, M., Shirasawa, T., 2008. AIJ guidelines for practical applications of CFD to pedestrian wind environment around buildings. J. Wind Eng. Ind. Aerodyn. 96, 1749–1761.
Tominaga, Y., Stathopoulos, T., 2007. Turbulent Schmidt numbers for CFD analysis with various types of flowfield. Atmos. Environ. 41, 8091–8099.
Tominaga, Y., Stathopoulos, T., 2013. CFD simulation of near-field pollutant dispersion in the urban environment: A review of current modeling techniques. Atmos. Environ. 79, 716–730.
Tominaga, Y., Yoshie, R., Mochida, A., Kataoka, H., Harimoto, K., Nozu, T., 2005. Cross Comparisons of CFD Prediction for Wind Environment at Pedestrian Level around Buildings. Part 2, 2661–2670.
Toparlar, Blocken, B, Vos, P, Janssen, W, van Hooff, T, Montazeri, H, Timmermans, H, 2015. CFD simulation and validation of urban microclimate: A case study for Bergpolder Zuid, Rotterdam. Build. Environ. Special Issue on Climate Adaption in Cities, Build. Environ., http://dx.doi.org/10.1016/j.buildenv.2014.08.004.
Van Hooff, T., Blocken, B., 2010. Coupled urban wind flow and indoor natural ventilation modelling on a high-resolution grid: a case study for the Amsterdam ArenA stadium. Environ. Model. Softw. 25, 51–65.
Vos, P.E., Maiheu, B., Vankerkom, J., Janssen, S., 2013. Improving local air quality in cities: To tree or not to tree? Environ. Pollut. 183, 113–122.
Wang, X., McNamara, K.F., 2006. Evaluation of CFD simulation using RANS turbulence models for building effects on pollutant dispersion. Environ. Fluid Mech. 6, 181–202.
Wieringa, J., 1992. Updating the Davenport roughness classification. J. Wind Eng. Ind. Aerodyn. 41, 357–368.
Wilson, N.R., Shaw, R.H., 1977. A higher order closure model for canopy flow. J. Appl. Meteorol. 16, 1197–1205.
Yoshie, R., Mochida, A., Tominaga, Y., Kataoka, H., Harimoto, K., Nozu, T., Shirasawa, T., 2007. Cooperative project for CFD prediction of pedestrian wind environment in the Architectural Institute of Japan. J. Wind Eng. Ind. Aerodyn. 95, 1551–1578.